RESTRICTED

THE COLLEGE OF AERONAUTICS
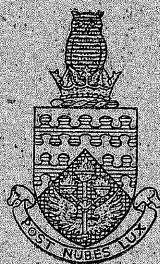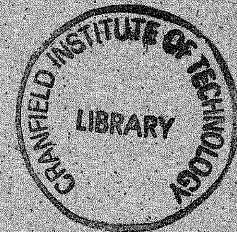
CRANFIELD

MEASUREMENTS OF LIFT, DRAG AND PITCHING MOMENT ON A LOW SPEED ROCKET FITTED WITH TAIL FINS OF VARIOUS SPANS

by

K. D. HARRIS and G. G. APPLEBY

THE   COLLEGE   OF   AERONAUTICS

CRANFIELD

Measurements of Lift, Drag and Pitching Moment on a
Low Speed Rocket fitted with Tail Fins of Various Spans

-by-

K.D. Harris, B.Sc.(Eng.), D.C.Ae., Grad.R.Ae.S.,

and

G.G. Appleby, B.Sc.(Eng.), A.C.G.I., D.I.C.

SUMMARY

Measurements of lift, drag and pitching moment have
been made in the No. 1A Wind Tunnel at the College of Aeronautics
at a speed of 132 f.p.s. on a model rocket supplied by the
Armament Research Establishment, Woolwich. The model was
tested with three different tail spans, and with no tail.

The tests made showed that the increase in static
stability was almost directly proportional to the net span of
the tail fins. For small angles of incidence the fin effective-
ness was the same for the fins mounted vertically and horizontally,
and for the fin assembly rotated through 45°. The model was
found to be statically stable about its point of suspension for
all three fin sizes, and no unsatisfactory characteristics were
observed over the test range of incidence from -12° to +18°.

The experimental results have been compared with
estimates based on slender body theory.

MEP

CONTENTS

Fig. (1) – Diagram of A.R.E. 2.35in. Rocket

(2) – Diagram of Fins

(3) – Diagram of Rig

(4) – C_L, C_D and C_m versus a – 1.7in. Fins

(5) – ' ' ' ' ' – 1.2in. Fins

(6) – ' ' ' ' ' – 0.83in. Fins

(7) – ' ' ' ' ' – No Fins

(8) – Comparison of Lift and Drag with different fins

(9) – Comparison of Pitching Moment with different fins

(10) – dC_m/da versus Fin Size.

(11) – Comparison of Theoretical and Experimental Results.

1. Notation

$$C_D = \frac{D}{\frac{1}{2}\rho V^2 S} = \text{Drag Coefficient}$$

$$C_L = \frac{L}{\frac{1}{2}\rho V^2 S} = \text{Lift Coefficient}$$

$$C_m = \frac{M}{\frac{1}{2}\rho V^2 S l} = \text{Pitching Moment Coefficient}$$

D =   Drag

d =   Maximum body diameter

L =   Lift

l =   Length of body

M =   Pitching moment about point of support of model

p_c =   Static pressure in settling chamber

p_A =   Atmospheric pressure

S =   Maximum cross-sectional area of body

S_b =   Base area of body

V =   Wind Speed

a =   Incidence of body axis to local free stream direction
        of flow

ρ =   Air density.

2. Introduction

This report gives the results of an investigation into the static stability characteristics of a model rocket supplied by the Armament Research Establishment, Woolwich. The investigation was made in the No. 1A open jet wind tunnel at the College of Aeronautics during April 1955.

About one year prior to these tests a similar set of tests was made in the No. 2 open jet wind tunnel at the College of Aeronautics on a model rocket of similar size, but of different nose and fin shape. These tests, in which the model was supported on a tail sting, were not entirely satisfactory, due, it was believed, to the fact that the moments were measured about a point far aft of the centre of pressure. In planning the present tests it was therefore decided to measure the pitching moment about the centre of gravity of the rocket, and to pay particular attention to the accuracy of the results.

The results obtained from the present set of tests are considered to be satisfactory. After applying a few simple correction factors, which are described later in this report, it was found that the results were very nearly symmetrical for positive and negative incidences, and that, to within the limits of experimental accuracy, the lift and pitching moment were in all cases zero at zero incidence.

3. Description of Apparatus

The tests were made in the No. 1A Wind Tunnel at the College of Aeronautics. This tunnel, which is of the open working section, return flow type, has an elliptic cross-section jet, 40in. wide by 27in. in depth.

The main lift balance is calibrated in grammes, but as rigged for the present test could only be read to within about ± 5 grammes. The drag balance is likewise calibrated in grammes and could also only be read to within about ± 5 grammes. The tail balance is calibrated in 0.002 lb. increments. Under the conditions of test the tail balance could just about be read to this limit of accuracy.

The model, which was full scale, is shown in Fig. 1. The body of the model was constructed of mahogany with steel inserts in the tailpiece and at the point of suspension. The tail fins, which are illustrated in Fig. 2, were made of gauge plate 0.048in. thick. The leading and trailing edges were left square.

The tail piece of the model was rotatable through 360°

about the longitudinal axis of the body. It was also detachable so that the different fin assemblies could be fitted into the tailpiece.

The method of suspension of the model is illustrated diagrammatically in Fig. 3. The model was suspended from the main lift balance by a streamlined steel strut having a thickness chord ratio of 15 per cent at the model end decreasing to 11 per cent at the balance end. The model was freely pivoted about this strut through a ball race. The incidence of the model could be adjusted by a worm operated winch on the tail balance.

4. Details of Test

The model was tested over the maximum obtainable range of incidence from $-12°$ to $+18°$. Measurements of lift, drag and pitching moment were taken for each of the three fin sizes, and on the body alone. The tests on the model with fins fitted were made with the fins:-

(a) horizontal and vertical ($+$), and

(b) at $45°$ to the vertical (X).

No transition wires were fitted to the fins, or to the body, for the fin on tests.

The tests on the body alone were made with and without a transition wire. The transition wire was attached to the body 3.2in. from the nose by means of a band of 'Cellotape'. The wire diameter was 0.028in.

When the results of these tests were initially plotted it was found that the lift and pitching moment curves did not pass through the origin. The following tests were therefore made to try and account for this unexpected result.

(i)   With each set of fins fitted in turn the fin assembly was rotated through $360°$ in increments of $45°$ at a time. Due presumably to small errors in manufacture, the pitching moment at nominally zero incidence was found to vary slightly as the fin assembly was rotated.

(ii)   The direction of flow was measured along the centre line of the working section using a Conrad type yawmeter. Assuming the yawmeter to have been accurately constructed it was found that the flow was inclined upwards by about 0.5 to 0.6 degrees to the horizontal.

(iii)   The zero readings of the balances were measured wind off and wind on. The observed values are tabulated below:-

$p_c - p_A$ (in.H_2O)	Lift Balance (gms).	Drag Balance (gms).	Tail Balance (lb.)
0	120	10	0.044
4	130	-5	0.038

When corrections were applied to the observed results for the above three effects it was found that the lift and pitching moment curves did then pass through the origin.

The incidence is considered accurate to within $\pm$ 0.2°. Neglecting tunnel interference corrections, which are uncertain but small, the lift coefficient is considered accurate to within $\pm$ 0.03, the drag coefficient to $\pm$ 0.02, and the pitching moment coefficient to $\pm$ 0.002. The faired curves are probably accurate to better than one half of these values.

5. Results

The fully corrected results are given in Table I. The corrections which have been applied to these results are (see para. 4):-

(i)   a correction to the observed incidence to give the true incidence relative to the local free stream direction,

(ii)   a correction to the observed pitching moment to allow for slight asymmetry of the model, and

(iii)   corrections to the observed lift, drag and pitching moment to allow for the change of the balance zero readings with wind on.

No corrections have been made for tunnel interference or for the interference effects of the strut and tail wire on the lift and pitching moment. The direct drag of the strut in the presence of the model has been measured and allowed for in the drag readings.

The results for each size of fin have been plotted in Figs. (4) to (6), and for the body alone in Fig. (7).

The curves obtained for each set of fins and the body alone
have been replotted in Figs. (8) and (9) to facilitate comparison
of the results. These curves are for the fins in the horizontal
and vertical positions only. In Fig. (10) the static stability,
measured by the quantity $-dC_m/d\alpha$ at $\alpha = 0^\circ$, is plotted against
the net span of the fins.

In Fig. (11) the experimental results have been
compared with estimates made using a combination of slender
body theory and lifting surface theory. An outline of the
method of estimation is given in Appendix I.

The main results of the test, and a comparison with
the estimated theoretical results, are given in the following
Table:-

Fins		1.7in.	1.2in.	0.83in.	No fins
$\left(\dfrac{dC_L}{d\alpha}\right)_{\alpha=0}$ per rad.	Experimental	8.37	6.60	4.87	2.01
	Theoretical	8.09	6.28	4.41	2.0
$\left(\dfrac{dC_m}{d\alpha}\right)_{\alpha=0}$ per rad.	Experimental	-1.55	-0.80	-0.12	0.80
	Theoretical				
Distance of Centre of Pressure aft of Pivot Point at $\alpha = 0^\circ$(ins.)	Experimental	3.67	2.40	0.50	-7.89
	Theoretical	2.87	1.44	-1.15	-8.95

6. Discussion

The fully corrected results given in Table I, and plotted
in Figs. (4) to (9), are considered accurate to within the limits
quoted in §4. It will be observed that all the lift and pitching
moment curves pass through the origin to within less than 0.2°.
The curves are also very nearly symmetrical for positive and
negative incidences. This suggests that little error can have
been introduced by neglecting the interference effect of the
supporting strut on the lift and pitching moment.

Referring to Figs. (4) to (6) it will be seen that for
small angles of incidence there appears to be a negligible
difference in the results obtained with the fins in the two
different positions. However, above about 5° incidence the fins
become progressively more effective when horizontal and vertical
than when rotated through 45°.

The body alone was tested with transition free, and with a transition wire 3.2in. from the nose. From Fig. (7) it will be seen that the transition wire had little effect on the $C_L \sim a$ curve up to nearly 10° incidence. On the other hand it did appear to have a slight stabilising effect on the $C_m \sim a$ curve; but the effect was so slight that it was not judged necessary to repeat the fin on tests with a transition wire attached to the body.

The static stability as measured by the quantity $- \dfrac{dC_m}{d a}$ at $a = 0^\circ$ is shown in Fig. (10) to be almost directly proportional to the net span of the fins. The model is statically stable for all three fin sizes, and there are no unsatisfactory characteristics over the test range of incidence from -12° to $+18^\circ$.

A comparison of the experimental results and estimates made by a combination of slender body theory and lifting surface theory is given in Fig. (11). In view of the crude assumptions made in deriving the theoretical results the agreement between theory and experiment is considered quite good. From the plot of $\left(dC_L / d a \right)_{a=0}$ it will be seen that the fins appear to be rather more effective than predicted by theory. Also, the centre of pressure appears to be from 1 to $1\frac{1}{2}$ inches aft of the theoretical value for all configurations. This kind of discrepancy is expected in the case of the body alone owing to the fact that slender body theory takes no account of the effects of viscosity. In the fin on cases the discrepancy between theory and experiment is also due partly to the neglect of viscosity. It is likely however that the discrepancy is due to other effects in addition. In view of this it is somewhat fortuitous that equally good agreement should have been obtained with theory in the fin on cases and the body alone case.

7. Conclusions

The tests have shown that the model was statically stable with all three fin sizes, and that there were no unsatisfactory characteristics over the test range of incidence from -12° to $+18^\circ$.

Comparison of the experimental results with theory shows that at zero incidence theory slightly underestimates the increment in lift curve slope due to the fins. Theory also underestimates the distance of the centre of pressure aft of the nose by about 1 to $1\frac{1}{2}$ inches for all configurations of the model.

APPENDIX I

Estimation of Lift Curve Slope and Centre of Pressure Position at zero Incidence

Body Alone

From slender body theory[1] the lift curve slope at zero incidence is

$$\left(\frac{\partial C_L}{\partial a}\right)_{a=0} = 2\,\frac{S_b}{S}$$

and the distance of the centre of pressure aft of the nose is

$$h_p = \frac{l}{d} - \frac{\text{Volume of Body}}{S_b \cdot d}$$

where, h_p = distance of centre of pressure aft of the nose (in units of maximum body diameter d).

Fins Alone

The lift curve slope of the fins alone was estimated from the Royal Aeronautical Society Data Sheets,[2] Wings S.01.03.03 and 04.

The centre of pressure position of the fins alone was assumed to be at the position predicted by slender body theory; namely,

$$x_{c.p.} = c_r - \frac{\int_{x=0}^{x=c_r} b^2 \cdot dx}{b_{T.E.}^2}$$

where,

x = distance aft of leading of wing root chord

$x_{c.p.}$ = distance of centre of pressure aft of leading edge of wing root chord
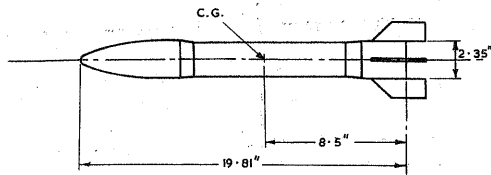
c_r = wing root chord

b = local net wing span

$b_{T.E.}$ = net wing span at trailing edge.

Body-Fin Combination

The lift curve slope and centre of pressure position of the body-fin combination were assumed to be given by the slender body theory formulae:-

$$\left(\frac{\partial C_L}{\partial a}\right)_{BW} = \left(\frac{\partial C_L}{\partial a}\right)_B + R_1 \left(\frac{\partial C_L}{\partial a}\right)_W$$

$$\left(x_{c.p.}\right)_{BW} = \frac{R_1 \left(\frac{\partial C_L}{\partial a}\right)_W (x_{c.p.})_W + \left(\frac{\partial C_L}{\partial a}\right)_B (x_{c.p.})_B}{R_1 \left(\frac{\partial C_L}{\partial a}\right)_W + \left(\frac{\partial C_L}{\partial a}\right)_B}$$

where, $\quad R_1 = \left(1 + \frac{d}{b}\right)^2$

$x_{c.p.} =$ distance of centre of pressure aft of any convenient reference point.

and $\quad$ suffix W refers to the wing alone

$\qquad$ ' $\quad$ B $\quad$ ' $\quad$ ' $\quad$ ' $\quad$ body $\quad$ '

$\qquad$ ' $\quad$ WB $\quad$ ' $\quad$ ' $\quad$ ' $\quad$ body-fin combination.

References

1. R.A.E. $\qquad$ Handbook of Supersonic Aerodynamic Data Applicable to Guided Weapon Design.

2. R.Ae.S. $\qquad$ Aerodynamics Data Sheets, Volume II.

TABLE OF RESULTS

		FINS AT 45°			FINS AT 90°		
	α	C_L	C_m	C_D	C_L	C_m	C_D
1.7in. Fins	-13	-1.92	0.427	0.74	-2.01	0.436	0.77
	-10	-1.43	0.320	0.57	-1.51	0.323	0.60
	- 7	-1.00	0.204	0.44	-1.08	0.205	0.47
	- 4	-0.53	0.104	0.37	-0.53	0.101	0.39
	- 1	-0.10	0.023	0.34	-0.09	0.017	0.34
	2	0.34	-0.062	0.37	0.34	-0.062	0.37
	5	0.79	-0.155	0.44	0.79	-0.155	0.44
	8	1.23	-0.257	0.54	1.25	-0.267	0.54
	11	1.77	-0.372	0.71	1.86	-0.382	0.74
	14	2.16	-I.463	0.84	2.29	-0.493	0.94
	17	2.63	-0.554	1.18	2.72	-0.600	1.24
1.2in. Fins	-13	-1.61	0.250	0.67	-1.67	0.272	0.71
	-10	-1.24	0.185	0.54	-1.30	0.193	0.54
	- 7	-0.90	0.120	0.44	-0.89	0.123	0.44
	- 4	-0.48	0.065	0.37	-0.46	0.063	0.37
	- 1	-0.18	0.015	0.34	-0.11	0.010	0.34
	2	0.18	-0.026	0.37	0.18	-0.037	0.37
	5	0.56	-0.079	0.44	0.54	-0.096	0.44
	8	0.92	-0.135	0.50	0.97	-0.155	0.50
	11	1.30	-0.206	0.62	1.36	-0.231	0.62
	14	1.65	-0.276	0.77	1.74	-0.317	0.84
	17	2.03	-0.344	1.01	2.17	-0.408	1.11
0.83in. Fins	-13	-1.17	0.100	0.59	-1.23	0.130	0.55
	-10	-0.86	0.063	0.45	-0.93	0.086	0.45
	- 7	-0.64	0.041	0.39	-0.66	0.055	0.40
	- 4	-0.34	0.016	0.35	-0.36	0.023	0.37
	- 1	-0.10	0	0.32	-0.11	0.004	0.34
	2	0.17	-0.014	0.35	0.16	-0.008	0.35
	5	0.41	-0.031	0.40	0.41	-0.031	0.40
	8	0.71	-0.056	0.47	0.72	-0.063	0.45
	11	0.97	-0.085	0.55	1.02	-0.095	0.55
	14	1.26	-0.124	0.69	1.33	-0.146	0.70
	17	1.58	-0.157	0.87	1.68	-0.193	0.89
	NO TRANSITION WIRE				0.028in. DIA. TRANSITION WIRE ATTACHED 3.2in. FROM NOSE		
No Fins	-13	-0.41	-0.175	0.47	-0.51	-0.162	0.54
	-10	-0.35	-0.130	0.40	-0.36	-0.127	0.47
	- 7	-0.25	-0.093	0.35	-0.25	-0.091	0.39
	- 4	-0.12	-0.046	0.34	-0.11	-0.054	0.35
	- 1	-0.02	-0.010	0.32	0	-0.017	0.34
	2	0.13	0.028	0.34	0.14	0.025	0.35
	5	0.19	0.077	0.35	0.20	0.064	0.37
	8	0.29	0.108	0.40	0.30	0.103	0.44
	11	0.39	0.148	0.44	0.42	0.134	0.47
	14	0.51	0.180	0.50	0.56	0.166	0.54
	17	0.64	0.200	0.60	0.71	0.195	0.64

C.G.

2·35"

8·5"

19·81"

SCALE: ¼.

DIAGRAM OF A.R.E. 2·35" ROCKET

FIG. 1.

1·7" FINS

1·7"

1·2" FINS

1·2"

0·83" FINS

45°   0·83"

2·08"   1·17"

DIAGRAM OF FINS

FIG. 2.

DRAG   MAIN LIFT   TAIL LIFT
BALANCE   BALANCE   BALANCE

DIAGRAM OF RIG

FIG. 3.

X FINS AT 45°
+ FINS AT 90°

C_D

1·0

0·5

-15   -10   -5   0   5   10   15   20
$\alpha°$

C_L C_m

2   0·4

1   0·2

-10   -5   5   10   15 $\alpha°$ 20

-1   -0·2

-2   -0·4

-3   -0·6

C_L

C_m
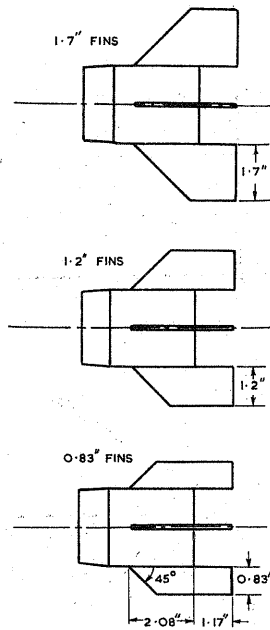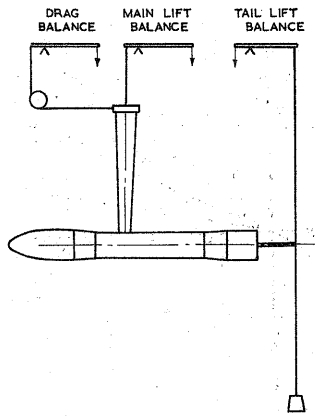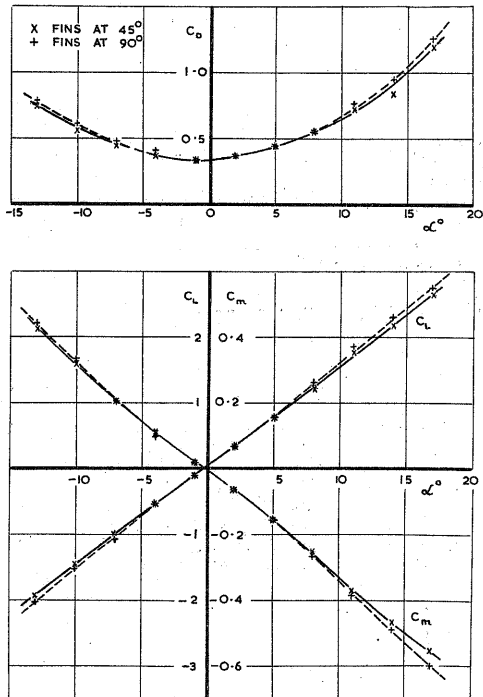
A.R.E. 2·35" ROCKET −1·7" FINS

FIG. 4.
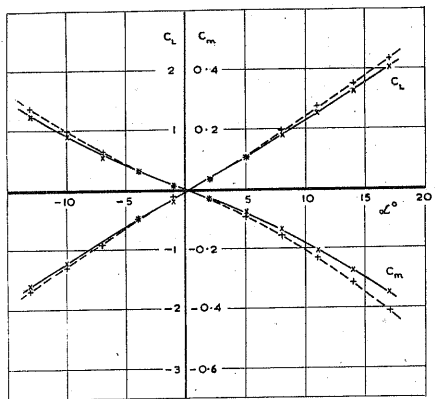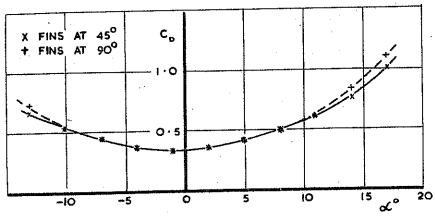
A.R.E. 2·35″ ROCKET – 1·2″ FINS
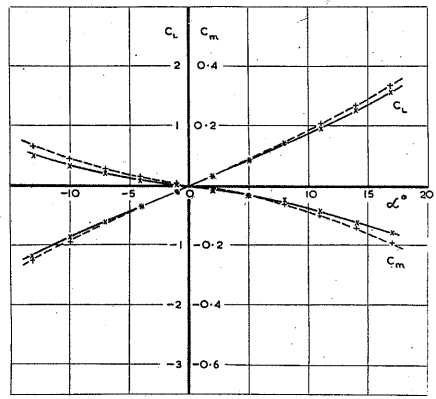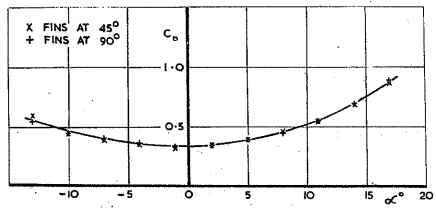
FIG. 5.
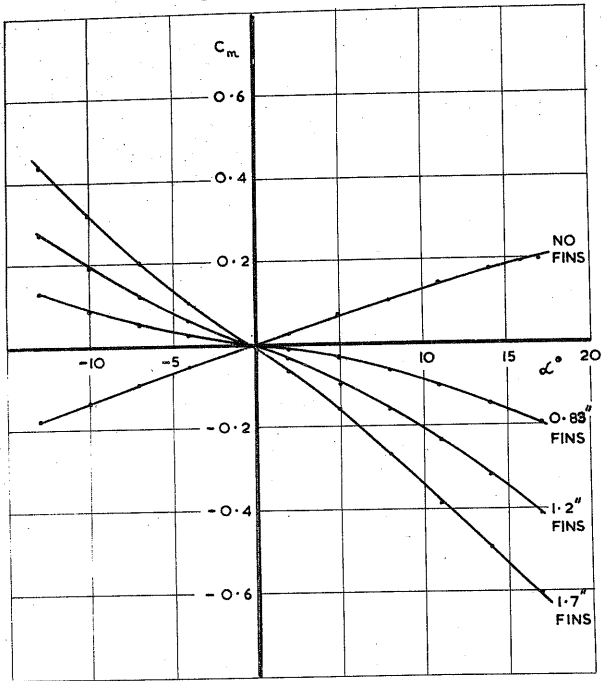

A.R.E. 2·35″ ROCKET – 0·83″ FINS

FIG. 6.
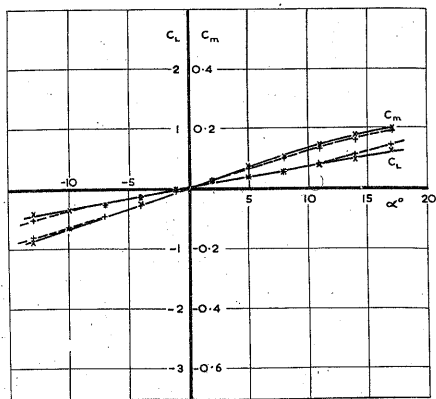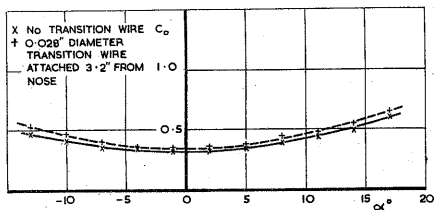
A.R.E. 2·35″ ROCKET – NO FINS
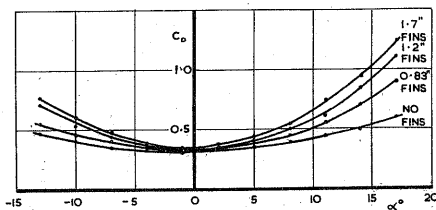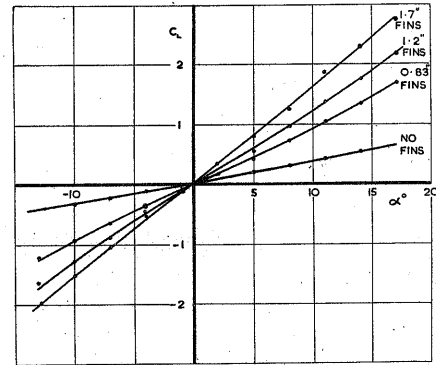
FIG. 7.

A.R.E. 2·35″ ROCKET – FINS AT 90°.
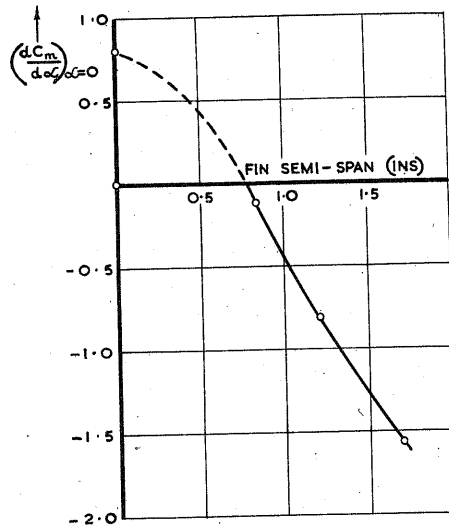
COMPARISON OF LIFT AND DRAG
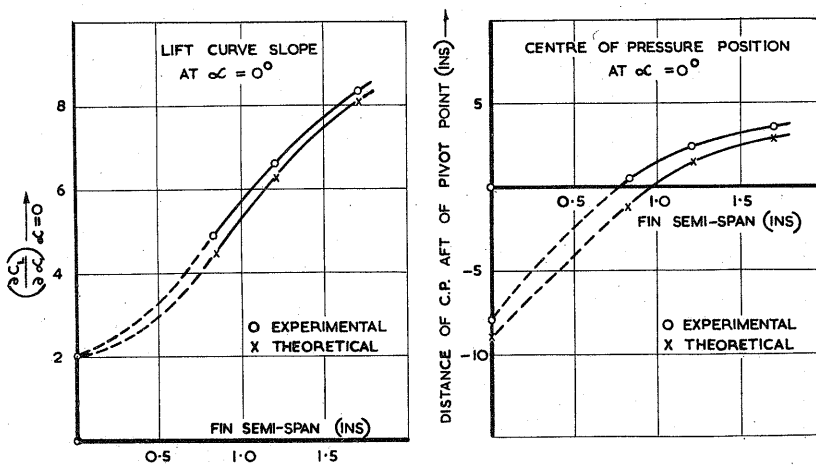WITH DIFFERENT FINS

FIG. 8.

A.R.E. 2·35" ROCKET-FINS AT 90°.
COMPARISON OF PITCHING MOMENT
WITH DIFFERENT FINS

FIG. 9.

STATIC STABILITY ~ FIN SIZE

FIG. 10.

COMPARISON OF THEORETICAL AND
EXPERIMENTAL RESULTS

FIG. 11.